RAPID COMMUNICATIONS

PHYSICAL REVIEW FLUIDS **2**, 082601(R) (2017)

Turbulent flow over a long flat plate with uniform roughness

D. I. Pullin
Graduate Aerospace Laboratories, California Institute of Technology, Pasadena, California 91125, USA

N. Hutchins and D. Chung
Department of Mechanical Engineering, University of Melbourne, Parkville, Victoria 3010, Australia

(Received 7 March 2017; published 31 August 2017)

For turbulent boundary-layer flow under a uniform freestream speed U_∞ over a plate of length L, covered with uniform roughness of nominal sand-grain scale k_s, the physical behaviors underlying two distinguished limits at large $\mathrm{Re}_L \equiv U_\infty L/\nu$ are explored: the fully rough wall flow where k_s/L is fixed and the long-plate limit where $\mathrm{Re}_k \equiv U_\infty k_s/\nu$ is fixed. For the fully rough limit it is shown that not only is the drag coefficient C_D independent of Re_L but that a universal skin-friction coefficient C_f and normalized boundary-layer thickness δ/k_s can be found that depends only on k_s/x, where x is the downstream distance. In the long-plate limit, it is shown that the flow becomes asymptotically smooth at huge Re_L at a rate that depends on Re_k. Comparisons with wind-tunnel and field data are made.

DOI: 10.1103/PhysRevFluids.2.082601

I. INTRODUCTION

The large-Reynolds-number limit for internal flows such as turbulent flow through a long rough-wall pipe are well characterized through the experiments of Nikuradse [1] and expressed via the Moody diagram [2]. For pipe and open-channel flow, when the flow is fully developed, turbulent, and fully rough in the sense that $k_s^+ \equiv k_s u_\tau/\nu$ (where k_s is the nominal sand-grain scale, $u_\tau = \sqrt{\tau_w/\rho}$, and τ_w is the wall drag per unit area for the rough surface) is sufficiently large, the time-averaged friction factor or skin-friction coefficient becomes asymptotically independent of Reynolds number at large values and depends only on the ratio of some measure of the roughness scale to either the pipe radius or the channel half height. Traditionally the concept of sand-grain roughness has been utilized for a given surface by determining an equivalent sand-grain roughness scale for which the skin-friction matches classical experimental sand-grain surface measurements [1]. For transitionally rough flows, where typically $70 > k_s^+ > 5$, the Hama [3] velocity correction can depend strongly on the surface roughness profile (see Ref. [4]).

There has been less attention on the effects of surface roughness at very large Reynolds number for canonical external flows such as the zero-pressure gradient flat plate boundary layer in the presence of uniform or variable roughness. For turbulent flow over a long flat plate of length L and freestream speed U_∞, calculations of the drag coefficient were reported by Prandtl and Schlichting [5,6]. They used a piecewise model of roughness variation with k_s^+ containing regions corresponding to smooth, transitional, and fully rough flow. The large $\mathrm{Re}_L \equiv U_\infty L/\nu$ limit has been subsequently considered by several authors [7–10]. Granville [7] found that for fixed k_s/x the integrated drag coefficient $C_D \equiv (1/L)\int_0^L C_f dx$ was independent of Re_L when this was large. The universality of mean-velocity profiles, skin friction, and some integral parameters for boundary layers over a variety of rough surfaces was studied analytically, assuming fully rough conditions, and experimentally by Castro [9]. Presently, we revisit this flow using an approach that is rather simpler than the methods of Prandtl and Schlichting and of Granville and is designed to provide an analytical interpretation of interesting and perhaps unexpected flow behavior in the large-Reynolds-number limit.

II. FLOW OVER A ROUGH FLAT PLATE

We consider flow of a turbulent boundary layer over a flat plate of length L with streamwise distance from the leading edge $0 \leqslant x \leqslant L$. The plate surface is covered with roughness whose height

distribution above a mean value $z = 0$ can be described as a random function of x and spanwise distance y that is isotropic and homogeneous. For the purposes of this analysis we consider the roughness to be characterized hydrodynamically by a single length scale k_s that is identified as the equivalent sand-grain roughness. In order to obtain an integrated description of smooth to fully rough wall flow, a Colebrook-type roughness function is used to describe the effects of roughness from the smooth through the transitional and fully rough-wall flow regimes. A principal parameter will be Re_L. This will be assumed to be sufficiently large that the prior laminar boundary layer and laminar-turbulent transition regions, typically in the range $0 \leqslant \mathrm{Re}_x \leqslant 5 \times 10^5$, can be ignored.

A. Mean velocity profile

We assume that the velocity profile within the boundary layer at any streamwise station x is given by the classical log-wake relationship

$$\frac{u}{u_\tau} = \frac{1}{\kappa}\ln\left(\frac{zu_\tau}{\nu}\right) + \frac{\Pi}{\kappa}W\left(\frac{z}{\delta}\right) - \Delta U^+\left(\frac{k_s u_\tau}{\nu}\right) + A, \tag{1}$$

where κ is the Kármán constant, z a suitably defined wall-normal distance, A an offset constant, W the wake function, and Π the Coles wake factor [11]. In Eq. (1), both u_τ and δ are functions of x and $\Delta U(k_s^+)$ is a roughness function that quantifies the effect of surface roughness on the mean velocity profile. Equation (1) does not include a description of the mean velocity variation in the viscous sublayer, the buffer layer, or a possible roughness sublayer. The contribution to mass and momentum transport across the whole boundary layer from these regions is expected to be small when Re_L is large and so will not be included in the analysis to follow. We assume a Colebrook form for transitionally rough conditions

$$\Delta U^+(k_s^+) = \frac{1}{\kappa}\ln(1 + \beta k_s^+). \tag{2}$$

When $k_s^+ \to \infty$ the choice $\beta = e^{\kappa(A-B)}$ allows matching to the usual fully rough form $\Delta U^+(k_s^+) = (1/\kappa)\ln(k_s^+) + A - B$.

The length scale δ is defined such that

$$S \equiv \frac{U_\infty}{u_\tau} \equiv \sqrt{\frac{2}{C_f}} = \frac{1}{\kappa}\ln\left(\frac{\delta u_\tau}{\nu}\right) + \frac{2\Pi}{\kappa} - \Delta U^+\left(\frac{k_s u_\tau}{\nu}\right) + A, \tag{3}$$

where $W(1) = 2$ by definition. For simplicity we use a simple model of the wake function $W(z/\delta) = 2\sin^2(\pi z/2\delta)$. Using $k_s u_\tau/\nu = (k_s/x)\mathrm{Re}_x/S$ and $\delta u_\tau/\nu \equiv \mathrm{Re}_\delta/S$, where $\mathrm{Re}_\delta \equiv U_\infty\delta/\nu$, $\mathrm{Re}_k \equiv U_\infty k_s/\nu$, and $\mathrm{Re}_x \equiv U_\infty x/\nu = \mathrm{Re}_k x/k_s$, we can solve for Re_δ from (3) as

$$\mathrm{Re}_\delta = Se^{\kappa(S-A)-2\Pi} + \mathrm{Re}_k e^{\kappa(S-B)-2\Pi}. \tag{4}$$

B. Momentum thickness and Kármán integral relation

The momentum thickness θ is

$$\theta = \int_0^\delta \frac{u}{U_\infty}\left(1 - \frac{u}{U_\infty}\right)dz. \tag{5}$$

Using (1) in Eq. (5) and integrating then gives

$$\mathrm{Re}_\theta = \mathrm{Re}_\delta(S)F(S), \quad F = \frac{\kappa S - 2 - \frac{3}{2}\Pi^2 + \Pi(\kappa S - Q)}{\kappa^2 S^2}, \tag{6}$$

where $Q = (2/\pi)[\pi + \mathrm{Si}(\pi)]$ and $\mathrm{Si}(\pi) \equiv \int_0^\pi [(\sin z)/z]dz = 1.851\,94$ and hence $Q = 3.178\,98$. As noted earlier, the above ignores the contribution of the viscous sublayer, the buffer layer, and/or a roughness sublayer.

For a zero pressure-gradient boundary layer, the Kármán integral relation can be written as

$$\frac{d\,\mathrm{Re}_\theta}{d\,\mathrm{Re}_x} = \frac{1}{S^2}, \tag{7}$$

where $\mathrm{Re}_\theta \equiv U_\infty \theta/\nu$. Considering $\mathrm{Re}_\theta = \mathrm{Re}_\theta[S(\mathrm{Re}_x)]$, using the chain rule for differentiation and (6), and integrating with Re_k and other parameters fixed, we find that

$$\mathrm{Re}_x - \mathrm{Re}_{x_0} = \int_{S_0}^{S} S'^2 \frac{d}{dS'}[\mathrm{Re}_\delta(S')F(S')]dS'. \tag{8}$$

The choice $S_0 = 0$ gives a divergent integral. At the cost of considerable complexity, this can be resolved by matching to a prior laminar boundary layer at some transition point $\mathrm{Re}_{x_0} = O(10^5)$. Instead, we use a simple cutoff $S_0 = O(1)$. Further, the contribution from the limit of integration $S = S_0$ can also be shown to be small when $\mathrm{Re}_x \gg O(10^5)$. Since this can be expected to have negligible effect on integrated quantities when $\mathrm{Re}_L = O(10^8)$, this will also be neglected. Alternative methods for handling the singularity have been used; see, for example, Ref. [9], Eq. (3.2).

Integrating (8) with Re_k fixed and neglecting the contribution from $S = S_0$, using $\mathrm{Re}_k = (k_s/x)\mathrm{Re}_x$ then gives

$$\mathrm{Re}_x = \frac{e^{\kappa(S-A)-2\Pi}}{\kappa^3} K_1(S) + \mathrm{Re}_x\left(\frac{k_s}{x}\right)\frac{e^{\kappa(S-B)-2\Pi}}{\kappa^2} K_2(S), \tag{9}$$

$$K_1 = \Pi^2\left(3 - \frac{3}{2}\kappa S\right) + \Pi[2 - 2\kappa S + \kappa^2 S^2 + Q(2 - \kappa S)] + (6 - 4\kappa S + \kappa^2 S^2), \tag{10}$$

$$K_2 = \left[\kappa S - 4 - \Pi(2 - \kappa S + Q) - \frac{3}{2}\Pi^2\right] + (4 + 2\Pi Q + 3\Pi^2)\mathrm{Ei}(\kappa S)e^{-\kappa S}, \tag{11}$$

where $\mathrm{Ei}(x) = -\int_{-x}^{\infty} e^{-t}/t\,dt$ is the exponential integral. If κ, A, B, and Π are specified, (9) provides a relation between $(\mathrm{Re}_x, k_s/x, S)$ or alternatively $(\mathrm{Re}_x, \mathrm{Re}_k, S)$. Calculations for specific cases are straightforward. All discussed subsequently were performed using the symbolic manipulator *Mathematica*, which provides special function capability for accurate calculation of $\mathrm{Ei}(x)$. As a check, some particular cases were calculated using asymptotic forms of $\mathrm{Ei}(x)$. Figure 1 shows resulting solutions from (9) for lines of constant Re_k (black curves) and lines of constant $\epsilon = k_s/x$ (blue curves) using $\kappa = 0.384$, $A = 4.17$, $B = 8.5$, and $\Pi = 0.53$.

Note that for a homogeneously distributed roughness of unvarying k_s along a flat plate, the black lines represent a fixed unit Reynolds number (U_∞/ν) and increasing x, while the blue curves represent a fixed x and increasing unit Reynolds number.

C. Drag coefficient

The drag coefficient for a plate of length L is

$$C_D = \frac{1}{L}\int_0^L C_f dx = \frac{1}{L}\int_0^L \frac{2}{S^2}dx = \frac{2}{\mathrm{Re}_L}\int_0^{\mathrm{Re}_L}\frac{1}{S^2}d\,\mathrm{Re}_x. \tag{12}$$

Using (7) this can be written in the form

$$C_D = \frac{2}{\mathrm{Re}_L}\int_0^{\mathrm{Re}_L}\frac{d\,\mathrm{Re}_\theta}{d\,\mathrm{Re}_x}d\,\mathrm{Re}_x = 2\frac{\mathrm{Re}_\theta(S_L)}{\mathrm{Re}_L}, \tag{13}$$

where we have used $\theta(x = 0) = 0$ and defined $S_L \equiv S(\mathrm{Re}_L)$. Utilizing (6) and again using that $\mathrm{Re}_k = (k_s/L)\mathrm{Re}_L$, we obtain an explicit formula for C_D,

$$C_D = 2\frac{1}{\mathrm{Re}_L}\left[S_L e^{\kappa(S_L-A)-2\Pi} + \mathrm{Re}_L\left(\frac{k_s}{L}\right)e^{\kappa(S_L-B)-2\Pi}\right]\frac{\kappa S_L - 2 - \frac{3}{2}\Pi^2 + \Pi(\kappa S_L - Q)}{\kappa^2 S_L^2}. \tag{14}$$

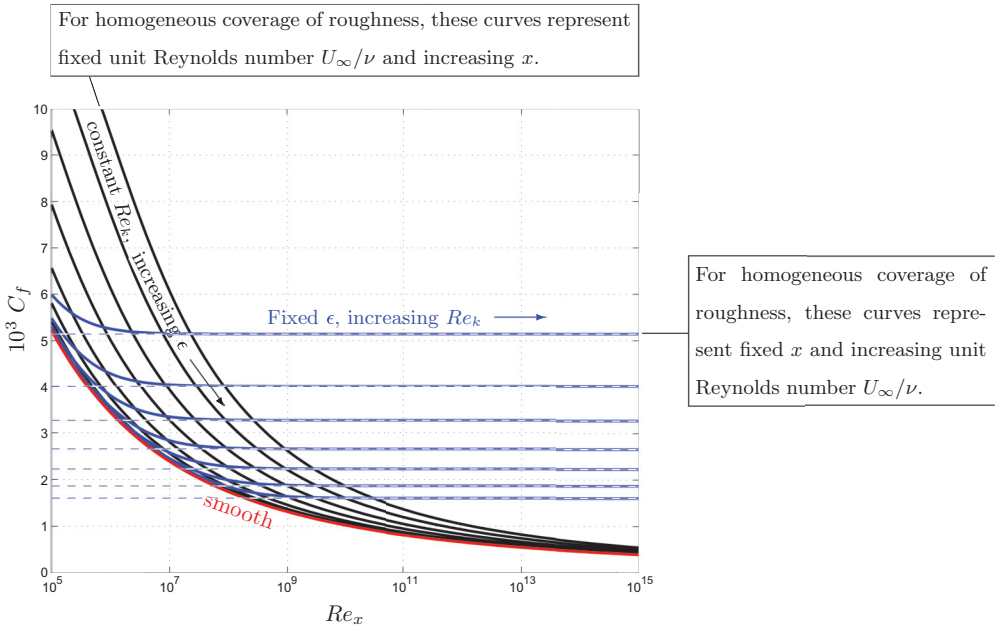

FIG. 1. Local friction coefficient C_f versus Re_x for fixed $\epsilon = k_s/x$ and fixed Re_k. Blue solid lines represent, from top to bottom, $\epsilon = 10^{-3}, 3\times10^{-4}, 10^{-4}, 3\times10^{-5}, 10^{-5}, 3\times10^{-6}, 10^{-6}$ and black lines, from top to bottom, $\mathrm{Re}_k = 3\times10^4, 10^4, 3\times10^3, 10^3, 3\times10^2, 10^2, 30$. The red curve shows the smooth wall ($\mathrm{Re}_k = 0$).

III. TWO LIMITING CASES

Two distinct limits are of interest. These are referred to as the fully rough-wall and long-plate limits, respectively. For most practical applications at large but finite $\mathrm{Re}_L = O(10^8$–$10^{10})$ and typical values of k_s/L, the rough-wall limit is of most interest. We consider the kinematic viscosity ν to be fixed.

A. Fully rough-wall flow

First let $\mathrm{Re}_x \to \infty$ by increasing the unit Reynolds number U_∞/ν at fixed ϵ. Here $\epsilon\,\mathrm{Re}_x \to \infty$ and the first term on the right-hand side of (9) can then be neglected. This gives the rough-wall limit

$$\frac{1}{\epsilon} \equiv \frac{x}{k_s} = \frac{e^{\kappa(S-B)-2\Pi}}{\kappa^2} K_2(S). \tag{15}$$

This equation shows explicitly that in the fully rough limit, S is a function of k_s/x only, or since $S^2 = 2/C_f$, the local skin-friction coefficient is only a function of k_s/x and is independent of Re_x. Solutions to (15) are plotted in Fig. 1 as blue dashed lines.

Similarly, the rough-wall limit of (4) can be taken by letting $\epsilon\,\mathrm{Re}_x \to \infty$ with ϵ fixed to give $\delta = k_s \exp[\kappa(S-B) - 2\Pi]$ or equivalently the well known form

$$S = \frac{1}{\kappa}\left[\ln\left(\frac{\delta}{k_s}\right) + 2\Pi\right] + B. \tag{16}$$

Recall that (15) has already shown that in the rough-wall limit, S (and hence C_f) is invariant with unit Reynolds number at fixed k_s/x (see the blue dashed curves in Fig. 1). Combining this result with (16) demonstrates that in the fully rough limit, for fixed k_s/x, δ/x must also be constant, i.e.,

$$\frac{\delta}{x} = \frac{\delta}{k_s}\left[S\left(\frac{k_s}{x}\right)\right]\frac{k_s}{x} = G\left(\frac{k_s}{x}\right), \tag{17}$$

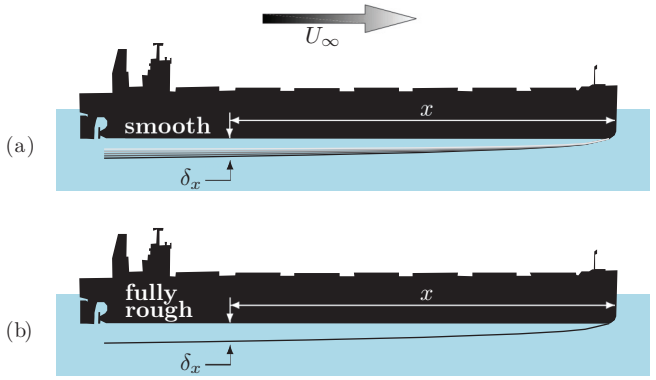

FIG. 2. Schematic demonstrating the development of the boundary layer along a hull for various different unit Reynolds numbers under (a) smooth and (b) fully rough conditions. Lighter shaded profiles denote higher freestream velocities. A homogeneously distributed roughness of constant k_s is assumed for the fully rough case. Boundary layer growth is exaggerated and indicative only.

where the square brackets here denote that δ/k_s is a function of the quantities inside the square brackets.

In practice, this suggests that for a flat plate (or, say, a ship's hull) homogeneously covered with roughness of height k_s, under fully rough conditions the boundary layer thickness at some fixed distance downstream from the leading edge δ must be invariant with unit Reynolds number. This result is somewhat counterintuitive, since for the smooth surface we know that δ remains a function of U_∞/ν. [Note that for the smooth wall, with $k_s/x = 0$ in Eq. (9), we find that S is a function of Re_x and hence from (3) with $\Delta U^+ = 0$ we see that δ is a function of x and Re_x.] This result is illustrated schematically for the ship case in Fig. 2. A smooth hull yields boundary layer profiles that are a function of freestream velocity [Fig. 2(a)], while under fully rough conditions the profiles are invariant with unit Reynolds number [Fig. 2(b)].

This result, while implicit in the work of Granville [7] (who shows that C_D depends only on L/k_s), is perhaps not widely known in the broad turbulence research community, but Eqs. (15) and (16) offer a succinct explicit demonstration of this. It is possible to find proof of this tendency in the literature. Figure 3 shows data from [12] for smooth and rough surfaces (P36 grit sandpaper). Figure 3(b) shows the boundary-layer thickness at $x = 21.7$ m downstream of the inlet to the working section ($\delta_{21.7}$) for both the smooth and rough surfaces as a function of the freestream velocity U_∞. Since the rough surface is not altered, these data are at fixed k_s/x. Note that for the smooth surface, the boundary-layer thickness at $x = 21.7$ m decreases as a function U_∞. However, for the rough surface, once the fully rough limit is approached [k_s^+ is shown in Fig. 3(a)], the boundary-layer thickness becomes invariant with unit Reynolds number (U_∞ in this case), confirming the result from (17). As a validation of the formulation presented here, the blue dashed line in Fig. 3 shows the corresponding numerical solutions obtained by letting $k_s/x = 1.96 \times 10^{-3}/21.7$ in Eqs. (9) and (4). It should be noted that the experiments of [12] are unique in the sense that (i) they studied a high-Reynolds-number boundary layer [we note from Fig. 1 that $\mathrm{Re}_x \approx O(10^7)$ is required to observe constant C_f at fixed k_s/x], (ii) they used an independent and accurate measurement of C_f using a floating plate drag balance, (iii) they had a sufficiently small blockage k/δ such that assumptions of outer layer similarity (and assumptions about the logarithmic form of the mean velocity profile) were unlikely to be violated, (iv) they employed testing at fixed x and multiple different unit Reynolds numbers U_∞/ν, and (v) they presented boundary-layer thickness data in tabulated form. However, there are other rough-wall studies in developing turbulent boundary layers where constant C_f as a function of Re_x can be approximately observed. Specifically, here we note that Schultz and Flack [13] show C_f becoming nominally constant with Re_x for both their uniform spheres and uniform spheres with grit cases and in these cases (particularly the latter) it is clear δ

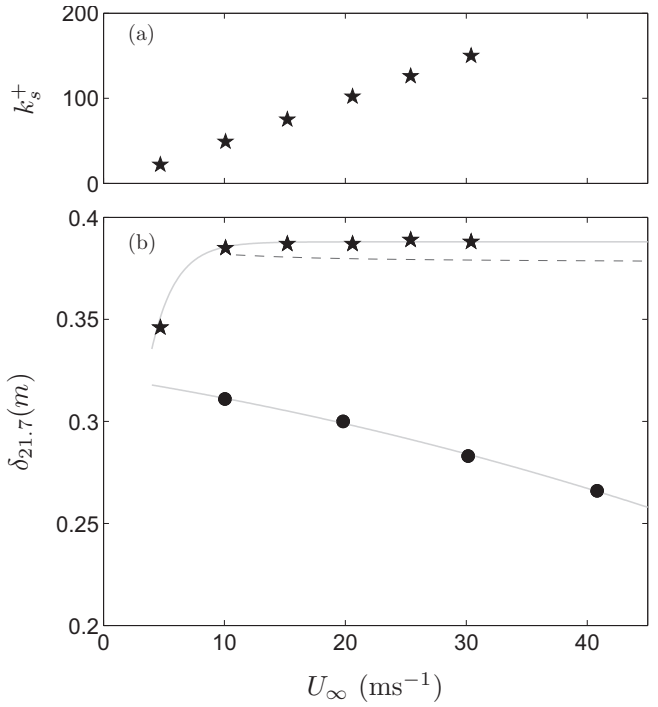

FIG. 3. (a) Plot of k_s^+ for the rough surface corresponding to U_∞. (b) Variation of boundary layer thickness at $x = 21.7$ m with freestream velocity as reported in Ref. [12] for the Melbourne University High Reynolds Number Boundary Layer Wind Tunnel for a rough test surface (stars), consisting of P36 grit sandpaper, with a determined $k_s = 1.96$ mm, and a smooth surface (circles). Gray curves show fits to the data. The dashed (gray) curve shows numerical solutions from (9) and (4) evaluated for $k_s/x = 1.96 \times 10^{-3}/21.7 = 9.03 \times 10^{-5}$.

seems to be tending to a constant (in particular when compared to the variation of δ with Re_x for the smooth surface). Similar tendencies are also observed for the 220-grit and 60-grit sandpapers studied by Schultz and Flack [14].

The fact that C_f and δ/k_s are both invariant with unit Reynolds number in the fully rough limit and for fixed k_s/x suggests that all mean velocity profiles under these conditions must collapse under the scaling z/k_s vs U^+. Figure 4 demonstrates this, showing with symbols the data from [12] at fixed k_s/x (fixed roughness $k_s = 1.96$ mm and $x = 21.7$ m) in the fully rough state $k_s^+ \gtrsim 70$, corresponding to $U_\infty = 15.2, 20.6, 25.4, 30.4$ ms^{-1}. The boundary layer thickness $\delta_{21.7}$ and k_s^+ corresponding to these freestream velocities were shown previously in Fig. 3. The solid lines show the mean profiles predicted from the previous calculations for matched conditions. These profiles are calculated by using $k_s/x = 1.96 \times 10^{-3}/21.7$ in Eq. (9), to yield S as a function of U_∞, which can then be used in Eq. (4) to obtain $\delta_{21.7}$ and hence in Eq. (1) to obtain the mean profiles. The results in Fig. 4 suggest very good collapse under this scaling. The only departures are where expected in the viscous near-wall-dominated profile that has not been modeled here.

For completeness, the integrated drag coefficient for the entire flat plate of length L can be calculated for the fully rough-wall case by substituting the limit $\mathrm{Re}_L \to \infty$ in Eq. (14) to give

$$C_D = 2\left(\frac{k_s}{L}\right) e^{\kappa(S_L - B) - 2\Pi} \frac{\kappa S_L - 2 - \frac{3}{2}\Pi^2 + \Pi(\kappa S_L - Q)}{\kappa^2 S_L^2}. \tag{18}$$

The solid blue and black curves in Fig. 5 show C_D as a function of Re_L for both constant Re_k and constant k_s/L, respectively, as calculated from (14). The blue dashed lines show the fully rough C_D as given by (18).

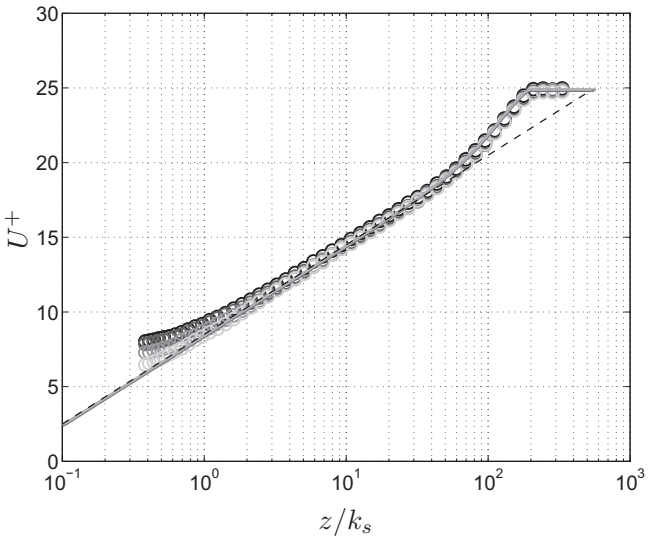

FIG. 4. Velocity profiles at constant k_s/x in the fully rough condition ($k_s^+ > 70$). Symbols show data from [12] at $x = 21.7$ m, for $U_\infty = 15.2, 20.6, 25.4, 30.4$ ms^{-1} corresponding to $k_s^+ > 70$. Lines show the mean profiles from the present calculations at matched conditions. Lighter shaded profiles and symbols denote higher freestream velocities. The dashed line shows $U^+ = \frac{1}{\kappa} \ln \frac{z}{k} + B$.

B. Long-plate limit

We now keep $\mathrm{Re}_k = \epsilon\, \mathrm{Re}_x$ fixed and let $x \to \infty$, corresponding to keeping the unit Reynolds number U_∞/ν and k_s fixed while increasing the plate length. We refer to this as the long-plate limit. It was recognized by Prandtl and Schlichting [5] from the trend of their numerical solutions, but they

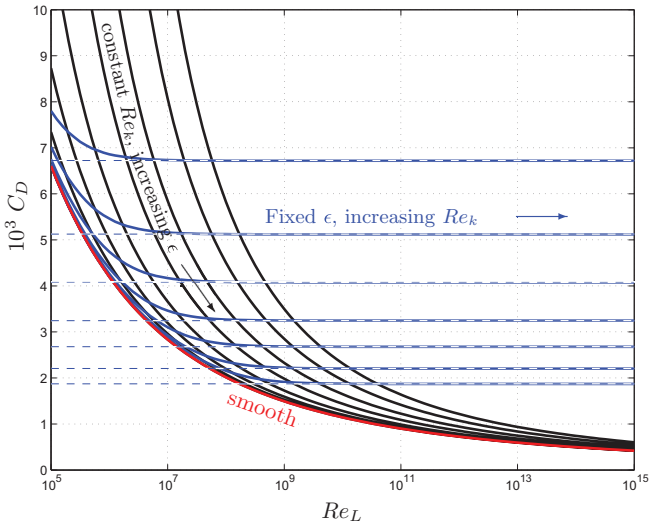

FIG. 5. Integrated drag coefficient C_D versus Re_L for fixed $\epsilon_L = k_s/L$ and fixed Re_k. Blue solid lines represent, from top to bottom, $\epsilon_L = 10^{-3}, 3\times10^{-4}, 10^{-4}, 3\times10^{-5}, 10^{-5}, 3\times10^{-6}, 10^{-6}$ and black lines, from top to bottom, $\mathrm{Re}_k = 3\times10^4, 10^4, 3\times10^3, 10^3, 3\times10^2, 10^2, 30$. The red curve shows the smooth wall ($\mathrm{Re}_k = 0$).

do not provide supporting analysis. The long-plate limit corresponds to moving along a hyperbola with fixed Re_k in the ϵ-Re_x plane: $\epsilon \to 0$ while $\mathrm{Re}_x \to \infty$ with both Re_k and the unit Reynolds number U_∞/ν remaining constant. It is then not clear *a priori* which term on the right-hand side of (9) becomes dominant when $\mathrm{Re}_x \to \infty$ and therefore whether either a smooth or rough-wall limit is approached. Using that $\mathrm{Ei}(x) \sim e^x/x$ when $x \to \infty$, for $S \gg 1$, (9) can be written as

$$\mathrm{Re}_x \sim \frac{e^{\kappa(S-A)-2\Pi}(1+\Pi)S^2}{\kappa} + \mathrm{Re}_k \frac{e^{\kappa(S-B)-2\Pi}(1+\Pi)S}{\kappa}. \tag{19}$$

The first term on the right-hand side is quadratic while the second term is linear in S. Hence, as Re_x is increased at fixed Re_k, S increases such that when $S > \mathrm{Re}_k$, the first term becomes dominant. This is sufficient to show that a smooth-wall limit is approached. An alternative interpretation is that $k_s^+ \equiv \mathrm{Re}_k/S$ decreases monotonically and eventually enters the sublayer when $k_s^+ \sim 5$. This then corresponds to a boundary layer, flowing over roughness of constant scale k_s, becoming asymptotically smooth when $x \to \infty$ at fixed U_∞/ν.

Figure 1 provides clear evidence of this long-plate limit. It is noted that all constant Re_k curves (black lines) are tending towards the smooth limit (red curve) at high Re_x. However, this limit is of little practical engineering relevance. If we consider the case of a ship operating at $U_\infty = 8.7\ \mathrm{ms}^{-1}$ and $\nu = 8.97 \times 10^{-7}\ \mathrm{m}^2\ \mathrm{s}^{-1}$ (as considered in Ref. [15]), we find that even for $\mathrm{Re}_k = 100$, corresponding to a very moderate fouling of $k_s \approx 10\ \mu$m, for the rough wall C_f to be within 2% of the smooth wall limit requires $\mathrm{Re}_x \approx 3.2 \times 10^{13}$ equating to a plate length in excess of 1000 km.

IV. CONCLUSION

Although implicit algebraic expressions were derived here for various quantities relevant to a turbulent boundary layer over a uniformly rough flat plate under a uniform freestream, the emphasis here was on interpreting the behavior of these quantities under two distinguished limits as $U_\infty L/\nu \to \infty$: (i) k_s/L fixed, called the fully rough limit, and (ii) $U_\infty k_s/\nu$ fixed, called the long-plate limit. While it is well appreciated that the drag coefficient C_D approaches a constant in the fully rough limit, it is perhaps underappreciated that both the local skin-friction coefficient C_f and the roughness-normalized boundary-layer thickness δ/k_s approach universal dependences on x/k_s. Physically, this behavior is easily observed when the boundary-layer thickness at a particular station approaches a constant with increasing freestream speed, an observation we showed to be corroborated by data in the literature. In the long-plate limit, it was shown that the flow approaches the behavior of a smooth wall, essentially because the skin friction, and hence the friction velocity, has decreased with downstream distance to a sufficiently small value such that $k_s u_\tau/\nu \lesssim 5$. However, very large Reynolds numbers are required to observe this limit.

ACKNOWLEDGMENT

This research was supported under Australian Research Council's Discovery Projects funding scheme (Grant No. DP160102279) and partially by NSF Award No. CBET 1235605.

[1] J. Nikuradse, 1933 Laws of flow in rough pipes, NACA Technical Memorandum 1292 (1950).
[2] L. F. Moody, Friction factors for pipe flow, Trans. Asme **66**, 671 (1944).
[3] F. R. Hama, Boundary layer characteristics for smooth and rough surfaces, Trans. Soc. Nav. Arch. Marine Engrs. **62**, 333 (1954).
[4] J. Jiménez, Turbulent flows over rough walls, Annu. Rev. Fluid Mech. **36**, 173 (2004).
[5] L. Prandtl and H. Schlichting, Das Widerstandsgesetz rauher Platten, Werft, Reederei, Hafen **15**, 4 (1934).
[6] L. Prandtl and H. Schlichting, The resistance law for rough plates, Department of Navy David Taylor Model Basin Report No. 258, 1955 (unpublished).

[7] P. S. Granville, The frictional resistance and turbulent boundary layer of rough surfaces, J. Ship Res. **2**, 52 (1958).
[8] J. C. Rotta, Turbulent boundary layers in incompressible flow, Prog. Aerosp. Sci. **2**, 1 (1962).
[9] I. P. Castro, Rough-wall boundary layers: Mean flow universality, J. Fluid Mech. **585**, 469 (2007).
[10] F. M. White, *Fluid Mechanics* (McGraw-Hill, New York, 2010).
[11] D. Coles, The law of the wake in the turbulent boundary layer, J. Fluid Mech. **1**, 191 (1956).
[12] D. T. Squire, C. Morrill-Winter, N. Hutchins, M. P. Schultz, J. C. Klewicki, and I. Marusic, Comparison of turbulent boundary layers over smooth and rough surfaces up to high Reynolds numbers, J. Fluid Mech. **795**, 210 (2016).
[13] M. P. Schultz and K. A. Flack, Outer layer similarity in fully rough turbulent boundary layers, Exp. Fluids **38**, 328 (2005).
[14] M. P. Schultz and K. A. Flack, Turbulent boundary layers over surfaces smoothed by sanding, J. Fluids Eng. **125**, 863 (2003).
[15] J. P. Monty, E. Dogan, R. Hanson, A. J. Scardino, B. Ganapathisubramani, and N. Hutchins, An assessment of the ship drag penalty arising from light calcareous tubeworm fouling, Biofouling **32**, 451 (2016).